Regular Article

Establishment and characterization of mouse bone marrow-derived mast cell hybridomas

Takeshi Kawahara*

Integrated Department of Sciences of Functional Foods, Graduate School of Agriculture, Shinshu University, Nagano, Japan

*Corresponding author: Integrated Department of Sciences of Functional Foods, Graduate School of Agriculture, Shinshu University, Nagano, Japan.

Fax: +81-265-77-1431.

E-mail: tkawafb@shinshu-u.ac.jp

Abstract

Interleukin (IL)-3-dependent mouse bone marrow-derived mast cells (BMMCs) are an important model for studying the function of mucosal-type mast cells. In the present study, BMMCs were successfully immortalized by cell fusion using a hypoxanthine-aminopterin-thymidine medium-sensitive variant of P815 mouse mastocytoma (P815-6TgR) as a partner cell line. The established mouse mast cell hybridomas (MMCHs) expressed α, β, and γ subunits of high-affinity immunoglobulin E (IgE) receptor (FcεRI) and possessed cytoplasmic granules devoid of or partially filled with electron-dense material. Four independent MMCH clones continuously proliferated without supplemental exogenous IL-3 and showed a degranulation response on stimulation with IgE + antigen. Furthermore, histamine synthesis and release by degranulation were confirmed in MMCH-D5, a MMCH clone that showed the strongest degranulation response. MMCH-D5 exhibited elevated levels of IL-3, IL-4, IL-13, granulocyte-macrophage colony-stimulating factor, tumor necrosis factor (TNF)-α, and cyclooxygenase 2, and production of prostaglandin D_2 and leukotriene C_4 in response to IgE-induced stimulation. MMCH clones also expressed Toll-like receptors (TLRs) 1, 2, 4, and 6 and showed elevated levels of TNF-α expression in response to stimulation with TLR2 and TLR4 ligands. The MMCHs established using this method should be suitable for studies on FcεRI- and TLR-mediated effector functions of mast cells.

Keywords: mast cell; cell fusion; P815; hybridoma; degranulation; Toll-like receptor

Abbreviations:

BMMC, mouse bone marrow-derived mast cell;

BSA, bovine serum albumin;

COX, cyclooxygenase;

DMSO, dimethyl sulfoxide;

DNP, dinitrophenol;

DNP-HSA, DNP-labeled human serum albumin;

FBS, fetal bovine serum;

FcεRI, high-affinity IgE receptor;

FITC, fluorescein isothiocyanate;

GAPDH, glyceraldehyde-3-phosphate dehydrogenase;

GM-CSF, granulocyte-macrophage colony-stimulating factor;

HAT, hypoxanthine-aminopterin-thymidine;

IgE, immunoglobulin E;

IL, interleukin;

LPS, lipopolysaccharide;

LT, leukotriene;

MC-CPA, mast cell carboxypeptidase A;

MMCH, mouse mast cell hybridoma;

NF-κB, nuclear factor-kappa B.

mMCP, mouse mast cell protease;

PBS, phosphate-buffered saline;

PE, phycoerythrin;

PG, prostaglandin;

RT-PCR, reverse transcription-polymerase chain reaction;

TLR, Toll-like receptor;

TNF, tumor necrosis factor.

INTRODUCTION

Mast cells are bone marrow-derived hematopoietic cells that play pivotal roles in immunoglobulin E (IgE)-associated immediate-type allergies. These cells are characterized by high-affinity IgE receptors (FcεRI) on their surface and many large cytoplasmic granules. Cross-linking of FcεRI by the interaction of FcεRI-bound IgE and specific multivalent antigen triggers 2 types of inflammatory immune reactions in mast cells. In the first reaction, which occurs within minutes, mast cells release presynthesized chemical mediators, including histamine and mast cell proteases stored in their granules [1–3]. Some released mediators immediately cause allergic symptoms such as a runny nose, sneezing, and asthma [4, 5]. In the second reaction, mast cells begin to produce proinflammatory cytokines and lipid mediators, including leukotriene (LT) C_4 and prostaglandin (PG) D_2 [6–8]. These newly synthesized agents lead to the development of severe and chronic allergic symptoms [9, 10].

In addition to their traditional roles in IgE-associated allergic reactions in the adaptive immune system, mast cells also participate in the innate immune system [11, 12]. Several Toll-like receptors (TLRs), which are highly conserved pattern-recognition receptors for pathogen-associated molecular patterns (PAMPs), are expressed in mast cells and have functional roles [13–15]. In particular, the role of TLR2 and TLR4 to recognize Gram-positive and Gram-negative bacterial components, respectively, and induce the production of proinflammatory cytokines such as tumor necrosis factor (TNF)-α and interleukin (IL)-6 has been extensively studied [13, 14, 16, 17].

The regulation of various mast-cell functions has been widely studied to understand their roles in the body or to develop novel therapeutic strategies against disorders involving them. For this purpose, many researchers have used IL-3-dependent mouse

bone marrow-derived mast cells (BMMCs) as a model. BMMCs are analogous to mucosal-type mast cells in ultra-structural and histochemical characteristics, and exhibit a variety of responses that reflect the fundamental roles of mast cells [18, 19]. However, the use of BMMCs is generally costly and time-consuming because they require IL-3 for sufficient differentiation (approximately 3–5 weeks) and subsequent survival and proliferation. Moreover, the viability of BMMCs is limited by senescence and eventual death within approximately 8–9 weeks in culture. In addition, BMMC cultures often include maturing cells in various stages of differentiation, making it impossible to exclude the influence of small numbers of other cell types during analyses. Therefore, the immortalization of BMMCs with mast-cell functions is considered an important strategy to overcome these difficulties. However, few studies have reported the immortalization of BMMCs with these functions using techniques other than the retroviral transformation method [20].

This report describes a method to artificially immortalize BMMCs using a cell fusion technique with a hypoxanthine-aminopterin-thymidine (HAT) medium-sensitive variant of the P815 mouse mastocytoma cell line. The resultant mouse mast cell hybridomas (MMCHs) proliferate well without supplemental IL-3 and are easily cloned. The 4 established MMCH clones expressed all subunits of FcεRI and showed a degranulation response to IgE-induced stimulation. Further analysis of the most IgE-reactive clone MMCH-D5 confirmed the release of histamine, elevated expression of proinflammatory genes, and production of LTC_4 and PGD_2. MMCHs also expressed TLR1, 2, 4, and 6 and responded to stimulation with TLR2 and TLR4 ligands.

MATERIALS AND METHODS

Cells and cell culture

The mouse mastocytoma cell line P815 was provided by the Institute for the Development of Aging and Cancer, Tohoku University (Miyagi, Japan). P815 cells were maintained in complete RPMI1640 medium (Nissui Pharmaceutical, Tokyo, Japan) supplemented with 10% fetal bovine serum (FBS; Equitech-Bio, Kerrville, TX, USA), 50 μM 2-mercaptoethanol, 100 IU/mL penicillin, and 100 μg/mL streptomycin in a humidified atmosphere of 5% CO_2/95% air at 37°C. To obtain the P815 cell variant with sensitivity to HAT medium containing 100 μM hypoxanthine, 0.4 μM aminopterin, and 16 μM thymidine, cells were treated with GIT medium (Nihon Pharmaceutical, Tokyo, Japan) with the addition of gradually increasing concentrations of 8-azaguanine (15–300 μM) followed by 6-thioguanine (10–50 μM). The resultant HAT-sensitive P815 cells, named P815-6TgR, were maintained in GIT medium containing 50 μM 6-thioguanine. P815 cells and P815-6TgR cells were preserved in liquid nitrogen using freezing medium containing 10% dimethyl sulfoxide (DMSO) and 20% FBS.

Mice

Specific pathogen-free female DBA/2 Cr mice were purchased from Japan SLC (Shizuoka, Japan) and housed at 23°C ± 3°C under a 12-h light/dark cycle. All animal protocols used in this study were approved by the Committee for Animal Experiments of Shinshu University.

Preparation and cultivation of BMMCs

BMMCs were prepared from 6–8-week-old mice according to a previously described method [21]. Briefly, mice were euthanized by cervical dislocation, and their intact

femurs were aseptically harvested. Bone marrow cells were obtained by repeatedly flushing the femurs with RPMI1640 medium containing 100 IU/mL penicillin and 100 μg/mL streptomycin. The cells thus obtained were washed twice with the same medium by centrifugation at 700 × *g* for 10 min. The centrifuged cells were suspended in complete RPMI1640 medium supplemented with 10% FBS, 0.1 mM nonessential amino acids (Gibco, Invitrogen, Grand Island, NY, USA), 5 ng/mL recombinant murine IL-3 (Peprotech, Rocky Hill, NJ, USA), 50 μM 2-mercaptoethanol, 100 IU/mL penicillin, and 100 μg/mL streptomycin. These cells were cultured at a density of 1×10^5 cells/mL in a humidified atmosphere of 5% CO_2/95% air at 37°C for 3–5 weeks until they differentiated into BMMCs.

Establishment and cultivation of MMCH clones

BMMCs were fused with P815-6TgR cells using the polyethylene glycol method. Separately cultured cells (3×10^6 cells) were suspended in GIT medium and mixed in a conical tube. After centrifugation at 300 × *g* for 10 min, precipitated cells were loosened and suspended in 0.3 mL of 50% polyethylene glycol (MW 4,000; Wako, Osaka, Japan) in phosphate-buffered saline (PBS; pH 7.2). After 1 min, 10 mL of GIT medium was gradually added to the tube. The suspension was centrifuged at 300 × *g* for 10 min, and the supernatant was discarded. The pellet was resuspended in GIT medium containing 5 ng/mL IL-3. One milliliter aliquots of the suspension at 6.0×10^4 cells/mL were transferred into tissue culture plates (Sarstedt, Newton, NC, USA). The culture was maintained by replacing the medium with fresh HAT medium containing 5 ng/mL of IL-3 until MMCH colonies appeared. The MMCHs were further cloned by limiting dilution. The resultant MMCH clones were maintained in GIT medium supplemented

with IL-3 (5 ng/mL).

To evaluate the effect of the concentration of DMSO in freezing medium on the viability of MMCHs, cells were preserved in liquid nitrogen using a freezing medium containing 0–10% DMSO and 40% FBS for 1 month.

Proliferation and viability of MMCHs were estimated by counting the cells using a hemocytometer in combination with a trypan blue exclusion test.

IgE-induced stimulation

For primary screening of IgE-reactive MMCHs, cells were suspended in fresh IL-3-supplemented GIT medium and sensitized with 5 μg/mL anti-dinitrophenol (DNP) mouse IgE (clone SPE-7; Sigma, St. Louis, MO, USA) for 24 h at 37 °C. After cultivation, the cells were washed with HEPES-Tyrode's buffer (137 mM NaCl, 5.6 mM glucose, 2.7 mM KCl, 0.5 mM NaH_2PO_4, 1.0 mM $CaCl_2$, and 10 mM HEPES at pH 7.3) containing 0.1% bovine serum albumin (BSA) and suspended in 150 μL of the same buffer. Cells were then stimulated with 50 μL (10 ng/mL final concentration) of DNP-labeled human serum albumin (DNP-HSA; Sigma) for 30 min at 37 °C.

For quantitative evaluation of degradation, MMCH-D5 cells, BMMCs, and P815-6TgR cells were washed with HEPES-Tyrode's buffer containing 0.1% BSA and suspended in 100 μL of the same buffer. The cell suspension (1×10^6 cells) was sensitized with the indicated concentrations of SPE-7 antibody for 2 h. After washing cells with HEPES-Tyrode's buffer, cells were stimulated with DNP-HSA for 30 min at 37°C.

β-Hexosaminidase release assay

IgE-induced degranulation was evaluated using a β-hexosaminidase release assay [22].

Briefly, 40 μL of the degranulation supernatant was transferred to a 96-well microtiter plate (Nunc; Thermo Fisher Scientific, Roskilde, Denmark) and incubated with 40 μL of 1 mM *p*-nitrophenyl-*N*-acetyl-D-glucosaminide (Sigma) in 0.1 M citrate buffer (pH 4.5) for 1 h at 37°C. The reaction was stopped by the addition of 160 μL of 0.1 M carbonate buffer (pH 10.0). The total β-hexosaminidase value was estimated by lysing the cells with 0.1% (w/v) Triton-X 100. The absorbance of the mixture was measured at 405 nm using a microplate reader (iMark; Bio-Rad, Hercules, CA, USA). The relative value of the β-hexosaminidase activity was calculated using the following formula: Degranulation (%) = {(S-N)/(T-N)} × 100, where S, N, and T represent absorbance value of supernatants obtained from IgE-treated cells, IgE-untreatedcells, and TritonX-100-treated cells, respectively.

Preparation of total RNA and reverse transcription-polymerase chain reaction (RT-PCR)

Total RNA was extracted from cells (2×10^6 cells) using TRIzol reagent (Invitrogen Life Technologies, Carlsbad, CA, USA) according to the manufacturer's protocol. The extracted RNA (1 μg) was reverse transcribed in a thermal cycler (PTC-200; MJ Research, Waltham, MA, USA) with 1 mM each dNTP, 2.5 units/μL M-MLV reverse transcriptase (Invitrogen), and 10 pmol/μL of oligo$(dT)_{18}$ primers at 42°C for 50 min. The resulting cDNA was subjected to semiquantitative or quantitative PCR. Semi-quantitative PCR using 1 μg of cDNA was performed using a *Taq* PCR Core Kit (Qiagen, Chatsworth, CA, USA) and 10 pmol/μL primers. Primer sequences were obtained from previous reports: FcεRI α and β [23], TLR1, 2, 4 and 6 [24], and glyceraldehyde-3-phosphate dehydrogenase (GAPDH) [25]. FcεRI γ primer sequences

5′-GTGGAACAAGCAGCCGCC-3′ (forward) and 5′-GAGATGGGGACCTGCCAGTG-3′ (reverse) from bases 81–98 and 480–460, respectively, were derived from GenBank accession number BC034163. The PCRs comprised 30 cycles of denaturation (94°C, 1 min), primer annealing (60°C, 1 min), and extension (72°C, 1 min), and were performed using the PTC-200. Amplified cDNAs were electrophoresed on 2% agarose gels in 0.04 M tris-acetate buffer (pH 8.0) containing 1 mM EDTA, and visualized by ethidium bromide staining. The fluorescent intensities of the bands were digitized using Printgraph software (Atto, Tokyo, Japan). Quantitative RT-PCR was performed using 0.5 μg of cDNA with a SYBR Premix Ex Taq (Takara Bio, Shiga, Japan) and 10 pmol/μL primers. Primer sequences were obtained from previous reports: mouse mast cell protease (mMCP)1, mMCP2, mMCP4–10, mast cell carboxypeptidase A (MC-CPA) [26], IL-4, IL-13, TNF-α, cyclooxygenase (COX)-2, and GAPDH [27]. IL-3 primer sequences, 5′-TGCCTACATCTGCGAATGAC-3′ (forward) and 5′-TTCCACGGTTAGGAGAGACG-3′ (reverse) from bases 320–339 and 487–468, respectively, were derived from GenBank accession number DQ788721. Granulocyte-macrophage colony-stimulating factor (GM-SCF) primer sequences, 5′-TAGCCAGGAGGGAGAACAGA-3′ (forward) and 5′-TGCATTCAAAGGGGATATCAG-3′ (reverse) from bases 418–438 and 579–559, respectively, were designed from GenBank accession number X02333. The PCRs comprised 1 cycle of preheating (95°C, 10 sec) and 45 cycles of denaturation (95°C, 5 sec), primer annealing (55°C, 10 sec), and extension (72°C, 20 sec) using a StepOnePlus Real Time PCR System (Life Technologies, Foster City, CA, USA). Results were analyzed with the ΔΔCt method using StepOne software (Life

Technologies). The amount of PCR products was normalized to the expression level of the GAPDH gene.

Flow cytometric analysis

Flow cytometric analysis was used to determine the cell surface expression of FcεRI and c-Kit of MMCH clones, BMMCs, and P815-6TgR cells. Cells (1×10^6 cells) were washed twice with PBS and treated with 0.125 μg/mL fluorescein isothiocyanate (FITC)-conjugated anti-mouse FcεRIα Armenian hamster IgG (clone MAR-1; eBioscience, San Diego, CA, USA) and 0.125 μg/mL phycoerythrin (PE)-conjugated anti-mouse c-Kit rat IgG (clone 2B8; eBioscience) at room temperature for 30 min. FITC-conjugated Armenian hamster IgG isotype control (clone eBio299Arm; eBioscience) and PE-conjugated rat IgG isotype control (clone eB149/10H5; eBioscience) were used for control staining under the same conditions. After treatment, the stained cells were washed once with PBS (pH7.2) and evaluated using FACSCalibur (BD Biosciences, San Jose, CA, USA). Data were analyzed using CellQuest Pro software (BD Bioscience).

Transmission electron microscopy

Suspensions of MMCH-D5, BMMC, and P815-6TgR cells were fixed with a mixture of 2% paraformaldehyde and 2.5% glutaraldehyde in PBS for 4 h at room temperature followed by further fixation with 1% osmium tetroxide for 1 h. After centrifugation at 3,000 rpm, an equal volume of 1% agarose was added to the pellet at 50°C. After cooling for solidification, the agarose-mixed samples were dehydrated in a graded series of ethanol followed by isopropyl alcohols. The dehydrated sample was embedded in an

epoxy resin and cut into 0.1-μm-thick sections with an OmU4 ultramicrotome (Reichert-Jung, Vienna, Austria). For electron microscopic observation, ultrathin sections were mounted on formvar-coated copper grids (VECO, Eerbeek, Netherlands), and doubly stained with uranyl acetate and lead citrate. The stained sections were viewed with a transmission electron microscope (JEM-1400; JEOL, Tokyo, Japan). Data were digitized with DigitalMicrograph software (Gatan, Pleasanton, CA, USA).

Enzyme-linked immunosorbent assay (ELISA)

A suspension (1×10^6 cells) of MMCH-D5 cells was collected and washed with HEPES-Tyrode's buffer containing 0.1% BSA. The cells were then simultaneously stimulated at 37 °C with or without the indicated concentrations of SPE-7 antibody and DNP-HSA in 200 μL of HEPES-Tyrode's buffer containing 0.1% BSA for the indicated durations. After incubation, the supernatant was collected by centrifugation at 10,000 × *g* for 5 min and stored at -80°C until needed. Levels of histamine, PGD_2, and LTC_4 in the supernatant were measured using the Histamine EIA kit (SPI-BIO, Montigny-le-Bretonneux, France), PGD_2 EIA Kit (Cayman Chemical, Ann Arbor, MI, USA), and LTC_4 EIA Kit (Cayman Chemical), respectively, in accordance with the manufacturer's recommendations.

TLR-mediated stimulation

MMCH clones, BMMCs, and P815-6TgR cells (2×10^6 cells) were harvested and seeded at 1×10^6 cells/mL in 48-well cell culture plates. The cells were stimulated with or without the indicated concentrations of Pam_3CSK_4 (InvivoGen, San Diego, CA, USA) or lipopolysaccharide (LPS) from *Salmonella enterica* serotype *typhimurium*

(Sigma) for 6 h. After cultivation, the cells were collected and washed once with ice-cold PBS. The washed cells were dissolved in TRIzol reagent and subjected to RT-PCR analysis.

Statistical analysis

Data were statistically analyzed using a two-tailed Tukey's multiple comparison test or Student's *t*-test. *P*-values less than 0.05 were considered statistically significant.

RESULTS

Establishment of a HAT medium-sensitive variant of P815 cells

P815 cells resistant to 300 μM 8-azaguanine were obtained after 1 month of treatment with increasing concentrations of 8-azaguanine. The surviving cells were further treated with 6-thioguanine. The resultant cells showed resistance to 50 μM 6-thioguanine stopped growing in HAT medium. The cells were further cloned by limiting dilution in medium containing 50 μM 6-thioguanine. One of the clones that showed the most vigorous proliferation was collected as a HAT-sensitive variant and named P815-6TgR.

Establishment of MMCH clones

After cultivating bone marrow cells in the presence of IL-3, over 94% of the non-adherent cells were identified as BMMCs by flow cytometric analysis of the cell surface expression of both FcεRI and c-Kit. The BMMCs were fused with P815-6TgR cells and cultured in HAT medium. Colonies formed by growing cells obviously larger than BMMCs appeared approximately 3–6 weeks after the fusion. The efficiency of BMMC and P815-6TgR cell fusion to establish MMCHs was estimated at

approximately 1 in 3.2×10^{-4} cells. Twelve MMCH clones were obtained by subsequent limiting dilution. The size of the MMCH clones was 18.7 ± 1.8 μm, which was larger than that of BMMCs (9.2 ± 0.9 μm) and P815-6TgR cells (14.2 ± 1.7 μm), under light microscopic observation.

Among the 12 MMCH clones, 6 clones were IgE-reactive clones that exhibited obvious β-hexosaminidase release in response to stimulation with IgE + antigen in the primary screening. However, the established clones showed limited survival after freezing in liquid nitrogen using a common freezing medium containing 10% DMSO and 20% FBS. Therefore, different concentrations of DMSO and FBS were tested to determine the optimum concentration in freezing medium for MMCHs was evaluated. After storage in liquid nitrogen for 1 month, the concentration of DMSO dramatically affected the viability of MMCHs preserved (**Fig. 1**). The viability of MMCHs increased to up to 34% as the concentration of DMSO was increased from 0% to 5%. On the other hand, concentrations of DMSO over 5% decreased the viability of MMCHs in a concentration-dependent manner. In particular, we verified the common freezing medium containing 10% DMSO notably diminished the viability of preserved MMCHs to 8%. In the presence of 5% DMSO, the concentration of FBS from 40% to 95% little affected cell viability (data not shown). Therefore, 5% DMSO and 40% FBS were established as the optimum concentrations, and freezing medium containing 5% DMSO and 40% FBS was employed for subsequent preservation of MMCHs. Eventually 4 clones (MMCH-A3, MMCH-A5, MMCH-C3, and MMCH-D5) were established through scale-up culture, cloning by limiting dilution, and repetitive freezing.

Protease expression profiles

The profiles of chymase (mMCP-1, 2, 4, and 5), tryptase (mMCP6–10), and MC-CPA expression in IgE-reactive MMCH clones are shown in **Fig. 2**. MMCHs showed strong expression of MC-CPA and mMCP-5, and weak expression of mMCP2, mMCP4, and mMCP6. BMMCs expressed mMCP2 in addition to MC-CPA, mMCP5, and mMCP6. P815-6TgR cells expressed low levels of expression of these proteases.

Growth and IL-3-dependence

All MMCH clones exhibited a logarithmic growth in the cell density range of 1×10^5–1×10^6 cells/mL (**Fig. 3**). Cell proliferation during 0–96 h of cultivation was not affected by the addition of exogenous IL-3. The viability of the MMCH clones remained at over 99% throughout the experimental period and was not affected by IL-3 supplementation (data not shown).

Expression of FcεRI and c-Kit

The intracellular mRNA levels of FcεRI α, β, and γ subunits in IgE-reactive MMCH clones, P815-6TgR cells, and BMMCs are shown in **Fig. 4A**. All the subunits of FcεRI were expressed in MMCH clones and BMMCs. Although P815-6TgR cells expressed γ subunits, they showed defective expression of α and β subunits.

Furthermore, the FcεRI α subunit was stained and subjected to flow cytometric analysis to confirm cell surface expression of FcεRI protein. The expression of FcεRIα was verified on all MMCH clones and BMMCs (**Fig. 4B**). Although the level of FcεRIα expression was different among the MMCH clones, it was obviously different from that of P815-6TgR cells, which had an undetectable level of FcεRIα on their surface. c-Kit expression was observed on all MMCH clones, P815-6TgR cells, and BMMCs.

Morphological features

The morphological characteristics of the MMCH-D5 clone, the clone that showed the most pronounced responsiveness to IgE-induced stimulation among the 4 established clones, were visualized by transmission electron microscopy and compared with those of BMMCs and P815-6TgR cells. The transmission electron micrographs indicated that these cells exhibited nuclei with partially condensed chromatin and short villi distributed regularly over the surface (**Fig. 5**). P815-6TgR cells had very few granule-like structures in their cytoplasm (**Fig. 5A**). Unlike P815-6TgR cells, MMCH-D5 clones contained many cytoplasmic granules devoid of or partially filled with an electron-dense matrix (**Fig. 5B**, **5C**, and **5D**). The granules of BMMCs appeared to be filled more completely with the matrix (**Fig. 5E** and **Fig. 5F**).

Degranulation and histamine release

Degranulation of the MMCH-D5 clone was quantitatively evaluated using serially diluted concentrations of IgE (0, 12.5, 25, 50, and 100 ng/mL) and antigen (0, 0.125, 0.25, 0.5, and 1 ng/mL). After stimulation, the MMCH-D5 clone released β-hexosaminidase in both an IgE- and antigen-dose-dependent manner, and the released value was calculated as 3–31% of the total value (**Fig. 6A** and **6B**). By contrast, P815-6TgR cells showed little responsiveness to this stimulation.

After 1 h of stimulation with IgE + antigen, the concentration of histamine in the supernatant from IgE-stimulated cells (254.8 ± 34.1 nM) was significantly higher than that from unstimulated cells (111.4 ± 28.6 nM) (**Fig. 6C**). The total histamine content of MMCH-D5 was estimated at 241.8 ± 37.4 ng/10^6 cells by measuring the histamine in

the supernatant obtained from Triton X-100-treated cells (data not shown). The proportion of the histamine released by stimulation was calculated as approximately 8% of the total histamine.

Expression of proinflammatory genes and production of lipid mediators

Elevation of mRNA expressions in the MMCH-D5 clone peaked at 2 h after stimulation and decreased within 4 h. **Fig. 7A** shows that the levels of IL-3, IL-4, IL-13, GM-CSF, TNF-α, and COX-2 in MMCH-D5 cells were elevated to 210%, 201%, 411%, 227%, 197%, and 649%, respectively, after stimulation with IgE + DNP-HSA for 2 h, and the increases were statistically significant compared to the levels in unstimulated cells.

The concentration of PGD_2 in the MMCH-D5 supernatant obtained after 1 h of IgE stimulation was 18.4 ± 0.5 pg/mL and was significantly higher than that of the unstimulated control (15.7 ± 0.6 pg/mL) (**Fig. 7B**). The increase in PGD_2 concentration was more pronounced in the supernatant obtained after 6 h of stimulation (unstimulated control, 16.9 ± 1.0 pg/mL; IgE-stimulated, 21.1 ± 1.0 pg/mL). The concentration of PGD_2 produced from IgE-stimulated and unstimulated cells after 6 h were 2.7 ± 0.1 pg/10^6 cells and 2.2 ± 0.1 pg/10^6 cells, respectively.

The concentration of LTC_4 was also significantly higher in the supernatants obtained from IgE-stimulated cells (1204.6 ± 101.0 pg/mL) compared to those from unstimulated cells (229.7 ± 125.6 pg/mL) (**Fig. 7C**). The concentrations of LTC_4 produced from IgE-stimulated and unstimulated cells were 154.2 ± 12.9 pg/10^6 cells and 29.4 ± 16.1 pg/10^6 cells, respectively.

Expression of TLRs and responsiveness to TLR-mediated stimulation

The expression of TLRs in MMCH clones is shown in **Fig. 8A**. All MMCH clones expressed TLR1, 2, 4, and 6. The expression levels of these TLRs were different among the clones. Treatment of the MMCH-D5 clone and BMMCs with ligands to TLR2 (1–100 μg/mL Pam_3CSK_4) and TLR4 (1–100 ng/mL LPS) induced TNF-α expression in a dose-dependent manner (**Fig. 8B**). In particular, the increase in TNF-α induced by Pam_3CSK_4 (10–100 μg/mL) and LPS (10–100 ng/mL) was statistically significant in both MMCH-D5 and BMMCs. Although P815-6TgR cells also expressed TLR1, 2, 4, and 6, they showed defective response to the ligands in the above-mentioned concentration ranges.

DISCUSSION

The cell fusion technique for obtaining hybridomas was initially described as a method for immortalizing plasma cells to produce monoclonal antibodies [28]. The immortalization is based on the transmission of infinite proliferative capacity from the neoplastic parent cell lines using fusion. This technique was thereafter also used to immortalize other immunocompetent cells [29–31]. However, MMCHs have not yet been reported because of the lack of an appropriate fusion partner cell line. This study is the first to report the successful establishment of functional BMMC hybridomas by cell fusion using P815 cells as a partner.

P815 cells are a methylcholanthrene-induced mastocytoma cell line originating from the DBAf/2 mouse [32]. Given the selection of hybridomas in HAT medium, original P815 cells were essentially unsuitable as fusion partner cells because they possess hypoxanthine-guanine phosphoribosyltransferase [33]. Therefore, prior to fusion, a HAT-sensitive variant was established by sequential drug selection with 8-azaguanine

and 6-thioguanine. After cultivation using these 2 purine analogs, the resultant P815-6TgR cells no longer grew in HAT medium, as described previously [34]. Although MMCHs established by this method required the determination of optimal DMSO concentration for freeze preservation (**Fig. 1**), 4 clones were eventually established as IgE-reactive clones. The clones principally expressed MC-CPA and mMCP-5 (**Fig. 2**). The expression pattern of mast cell proteases reflects the type of mast cells: mucosal type cells predominantly express mMCP1 and mMCP2, and connective tissue type cells express mMCP4, mMCP5, mMCP6, mMCP7, and MC-CPA [35]. IL-3-dependent BMMCs have been shown to express a unique protease expression pattern of MC-CPA, mMCP-5, and mMCP-6 despite their mucosal cell-like characteristics [35–38]. The expression pattern of mast cell proteases in MMCH clones was generally similar to that of BMMCs, except for mMCP2. Several reports have shown that the expression of mMCP2 is undetectable in IL-3-dependent BMMCs unless they are exposed to IL-9 and IL-10 [39, 40]. In addition to mMCP2, expression of proteases other than mMCP5 and MC-CPA was lower in MMCH clones compared to BMMCs. One possible reason for this decreased expression of proteases in MMCH clones may be the overall low levels of protease expression in P815-6TgR cells **(Fig. 2**). Thus, the protease expression in MMCH clones may be affected by the defective state of protease expression in P815-6TgR cells.

All the IgE-reactive MMCH clones survived and proliferated in the absence of exogenous IL-3 (**Fig. 3**). The IL-3-independence of MMCH clones is notably distinct from that of IL-3-dependent BMMCs. In this regard, P815 cells can survive in medium lacking IL-3 because they receive another survival signal from point-mutated c-Kit [41]. Therefore, MMCH clones presumably overcome IL-3 dependence by receiving the

survival signal of mutated c-Kit inherited from the P815-6TgR cells.

IgE-reactive MMCH clones expressed all FcεRI subunits in a manner similar that of BMMCs (**Fig. 4A**). By contrast, the expression of the FcεRI α and β subunits was absent in P815-6TgR cells. The expression of the FcεRIα subunit on the surface of MMCH clones and BMMCs was also confirmed by flow cytometric analysis (**Fig. 4B**). P815-6TgR cells lacked detectable expression of the α and β subunits of FcεRI, as reported for P815 cells [42]. In rodents, formation of αβγ2 tetramers of FcεRI is necessary for stable localization and function on the cell surface [43]. Therefore, IgE-reactive MMCH clones may inherit the ability to express FcεRI α and β subunits from BMMCs. Miller *et al.* reported that P815 cells transfected with both FcεRI α and β subunits failed to degranulate even after IgE stimulation [42]. Therefore, the IgE-induced degranulation reactivity of the MMCH clones is attributable to the recovery of not only FcεRI α and β subunits but also to other signaling components necessary for degranulation.

The degranulation ability of IgE-reactive MMCHs was also supported by transmission electron microscopic observations using MMCH-D5, the MMCH clone that exhibited the strongest reactivity to stimulation with IgE + antigen. MMCH-D5 exhibited mast cell-like features, including unsegmented nuclei, numerous narrow villi on the cell surface, and, in particular, many granules in the cytoplasm (**Fig. 5**). The granules of MMCH-D5 appeared immature compared to those of BMMCs because the granules contained a lesser amount of dense material. However, the existence of granules in MMCH-D5 cells was obviously distinct from that of P815-6TgR cells, which had only a few granules or none.

MMCH-D5 showed both IgE- and antigen-dose-dependent β-hexosaminidase release

(**Fig. 6A and 6B**). These results suggest that quantitative FcεRI-mediated signal transduction works in this clone. Therefore, the ability of MMCH-D5 to release histamine was investigated. As shown in **Fig. 6C**, the concentration of histamine in the MMCH-D5 supernatant significantly increased after stimulation with IgE + antigen, suggesting that MMCH-D5 released synthesized histamine by degranulation.

After 2 h of IgE + antigen stimulation, expression of IL-3, IL-4, IL-13, GM-CSF, and TNF-α was significantly elevated in MMCH-D5 (**Fig. 7A**). These proinflammatory cytokines increased after mast cell degranulation [44–47]. The significantly elevated expression of these cytokines suggests that IgE-induced signaling cascades are linked to the expression of these cytokines in MMCH-D5. **Fig. 7A** also shows that COX-2, an inducible synthase of PGs [48], was significantly upregulated in MMCH-D5 after stimulation. BMMCs produce PGD_2 as a major product of COX-2 following IgE-induced degranulation [49]. Indeed, PGD_2 production from MMCH-D5 after both 1 and 6 h of stimulation with IgE, mainly corresponding to COX-2-independent and COX-2-dependent production of PGD_2, respectively [50, 51], was significantly increased (**Fig. 7B**). Furthermore, production of the other major arachidonic acid mediator metabolite LTC_4 was more notably induced by IgE + antigen stimulation (**Fig. 7C**). Razin *et al.* [52] reported that IL-3-dependent BMMCs produce LTC_4 in marked preference to PGD_2. Therefore, vigorous synthesis of LTC_4 rather than PGD_2 from MMCH-D5 may reflect the properties of BMMCs used in this study.

In addition to the reactivity of FcεRI, MMCH clones expressed TLR1, 2, 4, and 6 (**Fig. 8A**). The expression of TLRs in MMCHs was common to BMMCs and P815-6TgR cells. Recent studies showed that BMMCs express TLR2, 4, and 6 [7, 9]. The expression of TLR1 in both MMCHs and BMMCs was confirmed. TLR1 and TLR6

associated with TLR2 for expanded ligand recognition without generating differential signaling [53]. The expression patterns of TLRs in MMCH clones suggest that TLR2 and TLR4 signaling pathways are active in MMCHs. As expected, TNF-α expression was significantly elevated in MMCH-D5 by Pam_3CSK_4 and LPS stimulation (**Fig. 8B**), suggesting that TLR2- and TLR4-mediated signaling pathways are active in the established MMCHs. Furthermore, the tripalmitoylated lipopeptide Pam_3CSK_4 is recognized by the cooperation of TLR1 and TLR2 and leads to the activation of nuclear factor-kappa B (NF-κB) [54]. The elevation of TNF-α expression in MMCHs and BMMCs by Pam_3CSK_4 stimulation is consisted with their TLR expression and suggests that the TLR1 on these cells activates the NF-κB signaling pathway.

To date, few spontaneously established mouse mast cell lines that can serve as mast cell models have been reported [55]. Although the mast cell model provides much meaningful information, there are practical difficulties in conducting studies using a large number of mast cells because of their requirement for precious growth factors similar to the case of BMMCs [55]. This study demonstrates the generation of MMCHs by fusion of BMMCs and P815-6TgR cells. MMCHs grew in the absence of IL-3 and exhibited some characteristics similar to those of BMMCs. In particular, MMCHs express FcεRI and TLRs and show fundamental response to stimulation. However, it should be noted that MMCH clones may not be exactly equivalent to BMMCs because the former may harbor constitutively active c-Kit. If this issue is addressed, potential advantages derived from the properties of MMCHs should be useful. The method used in this study to establish MMCHs may serve to overcome such difficulties and facilitate studies on some of the FcεRI- and TLR-mediated effector functions of mast cells.

ACKNOWLEDGMENTS

This work was supported by a Grant-in-Aid for Scientific Research from the Japan Society for the Promotion of Science (JSPS). This research was also supported in part by the Japan Science and Technology Agency (JST).

I would like to express my sincere gratitude to my supervisor, Professor Hajime Otani, of the Laboratory of Food Bioscience, Graduate School of Agriculture, Shinshu University, for providing me the encouragement and the opportunity to study in his laboratory. This work was technically supported by the Research Center for Human and Environmental Sciences Division of Instrumental Analysis, Shinshu University and the Collaborated Research Center for Food Functions, Faculty of Agriculture, Shinshu University.

REFERENCES

[1] D.D. Metcalfe, D. Baram, Y. A. Mekori, Mast cells, Physiol. Rev. 77, (1997) 1033–1079.

[2] S.J. Galli, Mast cells and basophils, Curr. Opin. Hematol. 7, (2000) 32–39.

[3] C.M. Williams, S.J. Galli, The diverse potential effector and immunoregulatory roles of mast cells in allergic disease, J. Allergy Clin. Immunol. 105, (2000) 847–859.

[4] G. Marone, M. Triggiani, A. Genovese, A.D. Paulis, Role of human mast cells and basophils in bronchial asthma, Adv. Immunol. 88, (2005) 97–160.

[5] S.J. Galli, J. Kalesnikoff, M.A. Grimbaldeston, A.M. Piliponsky, C.M. Williams, M. Tsai, Mast cells as ‘‘tunable’’ effector and immunoregulatory cells: recent

advances, Annu. Rev. Immunol. 23, (2005) 749–786.

[6] M. Metz, M.A. Grimbaldeston, S. Nakae, A.M. Piliponsky, M. Tsai, S.J. Galli, Mast cells in the promotion and limitation of chronic inflammation, Immunol. Rev. 217, (2007) 304–328.

[7] H.S. Kuehn, E.J. Swindle, M.S. Kim, M.A. Beaven, D.D. Metcalfe, A.M. Gilfillan, The phosphoinositide 3-kinase-dependent activation of Btk is required for optimal eicosanoid production and generation of reactive oxygen species in antigen-stimulated mast cells, J. Immunol. 181, (2008) 7706–7712.

[8] E. Razin, J.M. Mencia-Huerta, R.L. Stevens, R.A. Lewis, F.T. Liu, E. Corey, K.F. Austen, IgE-mediated release of leukotriene C_4, chondroitin sulfate E proteoglycan, beta-hexosaminidase, and histamine from cultured bone marrow-derived mouse mast cells, J. Exp. Med. 157, (1983) 189–201.

[9] T. Satoh, R. Moroi, K. Aritake, Y. Urade, Y. Kanai, K. Sumi, H. Yokozeki, H. Hirai, K. Nagata, T. Hara, M. Utsuyama, K. Hirokawa, K. Sugamura, K. Nishioka, M. Nakamura, Prostaglandin D_2 plays an essential role in chronic allergic inflammation of the skin via CRTH2 receptor, J. Immunol. 177, (2006) 2621–2629.

[10] N.A. Soter, R.A. Lewis, E.J. Corey, K.F. Austen, Local effects of synthetic leukotrienes (LTC_4, LTD_4, LTE_4, and LTB_4) in human skin, J. Invest. Dermatol. 80, (1983) 115–119.

[11] R. Malaviya, T. Ikeda, E. Ross, S.N. Abraham, Mast cell modulation of neutrophil influx and bacterial clearance at sites of infection through TNF-α, Nature 381, (1996) 77–80.

[12] T. Jippo, E. Morii, A. Ito, Y. Kitamura, Effect of anatomical distribution of mast

cells on their defense function against bacterial infections: demonstration using partially mast cell-deficient tg/tg mice, J. Exp. Med. 197, (2003) 1417–1925.

[13] V. Supajatura, H. Ushio, A. Nakao, K. Okumura, C. Ra, H. Ogawa, Protective roles of mast cells against enterobacterial infection are mediated by Toll-like receptor 4, J. Immunol. 167, (2001) 2250–2256.

[14] J.D. McCurdy, T.J. Lin, J.S. Marshall, Toll-like receptor 4-mediated activation of murine mast cells, J. Leukoc. Biol. 70, (2001) 977–984.

[15] H. Matsushima, N. Yamada, H. Matsue, S. Shimada, TLR3-, TLR7-, and TLR9-mediated production of proinflammatory cytokines and chemokines from murine connective tissue type skin-derived mast cells but not from bone marrow-derived mast cells, J. Immunol. 173, (2004) 531–541.

[16] J.D. McCurdy, T.J. Olynych, L.H. Maher, J.S. Marshall, Cutting edge: distinct Toll-like receptor 2 activators selectively induce different classes of mediator production from human mast cells, J. Immunol. 170, (2003) 1625–1629.

[17] E. Rönnberg, B. Guss, G. Pejler, Infection of mast cells with live streptococci causes a Toll-like receptor 2- and cell-cell contact-dependent cytokine and chemokine response, Infect Immun. 78, (2010) 854–864.

[18] E. Razin, C. Cordon-Cardo, R.A. Good, Growth of a pure population of mouse mast cells in vitro with conditioned medium derived from concanavalin A-stimulated splenocytes, Proc. Natl. Acad. Sci. USA. 78, (1981) 2559–2561.

[19] J.W. Schrader, S.J. Lewis, I. Clark-Lewis, J.G. Culvenor, The persisting (P) cell: histamine content, regulation by a T cell-derived factor, origin from a bone marrow precursor, and relationship to mast cells, Proc. Natl. Acad. Sci. USA. 78, (1981) 323–327.

[20] N. Arora, K.U. Min, J.J. Costa, J.S. Rhim, D.D. Metcalfe, Immortalization of mouse bone marrow-derived mast cells with Ad12-SV40 virus, Int. Arch. Allergy Immunol. 100, (1993) 319–327.

[21] E. Lee, J. Yook, K. Haa, H.W. Chang, Induction of Ym1/2 in mouse bone marrow-derived mast cells by IL-4 and identification of Ym1/2 in connective tissue type-like mast cells derived from bone marrow cells cultured with IL-4 and stem cell factor, Immunol. Cell Biol. 83, (2005) 468–474.

[22] F. Shinomiya, Y. Hamauzu, T. Kawahara, Anti-allergic effect of a hot-water extract of quince (*Cydonia oblonga*), Biosci. Biotechnol. Biochem. 73, (2009) 1773–1778.

[23] M.C. Jamur, A.C. Grodzki, E.H. Berenstein, M.M. Hamawy, R.P. Siraganian, C. Oliver, Identification and characterization of undifferentiated mast cells in mouse bone marrow, Blood 105, (2005) 4282–4289.

[24] G. Soboll, L. Shen, C.R. Wira, Expression of Toll-like receptors (TLR) and responsiveness to TLR agonists by polarized mouse uterine epithelial cells in culture, Biol. Reprod. 75, (2006) 131–139.

[25] K. Tobita, T. Kawahara, H. Otani, Bovine beta-casein (1-28), a casein phosphopeptide, enhances proliferation and IL-6 expression of mouse $CD19^+$ cells via Toll-like receptor 4, J. Agric. Food Chem. 54, (2006) 8013–8017.

[26] J. Kashiwakura, W. Xiao, J. Kitaura, Y. Kawakami, M. Maeda-Yamamoto, J.R. Pfeiffer, B.S. Wilson, U. Blank, T. Kawakami, Pivotal advance: IgE accelerates in vitro development of mast cells and modifies their phenotype, J. Leukoc. Biol. 84, (2008) 357–367.

[27] T. Kawahara, Inhibitory effect of heat-killed *Lactobacillus* strain on

immunoglobulin E-mediated degranulation and late-phase immune reactions of mouse bone marrow-derived mast cells, Anim, Sci, J. 81, (2010) 714–721.

[28] G. Köhler, C. Milstein, Continuous cultures of fused cells secreting antibody of predefined specificity, Nature 256, (1975) 495–497.

[29] M. Okada, N. Yoshimura, T. Kaieda, Y. Yamamura, T. Kishimoto, Establishment and characterization of human T hybrid cells secreting immunoregulatory molecules, Proc. Natl. Acad. Sci. USA. 78, (1981) 7717–7721.

[30] E. Tzehoval, S. Segal, N. Zinberg, M. Feldman, Macrophage-hybridomas: generation, structure, and function, J. Immunol. 132, (1984) 1741–1747.

[31] R.C. Chan, H. Xie, G.P. Zhao, Y. Xie, Dendritomas formed by fusion of mature dendritic cells with allogenic human hepatocellular carcinoma cells activate autologous cytotoxic T lymphocytes, Immunol. Lett. 83, (2002) 101–109.

[32] T.B. Dunn, M. Potter, A transplantable mast-cell neoplasm in the mouse, J. Natl. Cancer Inst. 18, (1957) 587–601.

[33] F. Benchetrit, A. Ciree, V. Vives, G. Warnier, A. Gey, C. Sautès-Fridman, F. Fossiez, N. Haicheur, W.H. Fridman, E. Tartour, Interleukin-17 inhibits tumor cell growth by means of a T-cell-dependent mechanism, Blood 99, (2002) 2114–2121.

[34] M.B. Meyers, O.P. van Diggelen, M. van Diggelen, S. Shin, Isolation of somatic cell mutants with specified alterations in hypoxanthine phosphoribosyltransferase, Somatic Cell Genet. 6, (1980) 299–306.

[35] G. Pejler, M. Abrink, M. Ringvall, S. Wernersson, Mast cell proteases, Adv. Immunol. 95, (2007) 167–255.

[36] D.S. Reynolds, R.L. Stevens, D.S. Gurley, W.S. Lane, K.F. Austen, W.E. Serafin, Isolation and molecular cloning of mast cell carboxypeptidase A. A novel member

of the carboxypeptidase gene family, J. Biol. Chem. 264, (1989) 20094–20099.

[37] D.S. Reynolds, D.S. Gurley, K.F. Austen, W.E. Serafin, Cloning of the cDNA and gene of mouse mast cell protease-6. Transcription by progenitor mast cells and mast cells of the connective tissue subclass, J. Biol. Chem. 266, (1991) 3847–3853.

[38] H.P. McNeil, K.F. Austen, L.L. Somerville, M.F. Gurish, R.L. Stevens, Molecular cloning of the mouse mast cell protease-5 gene. A novel secretory granule protease expressed early in the differentiation of serosal mast cells, J. Biol. Chem. 266, (1991) 20316–20322.

[39] N. Ghildyal, H.P. McNeil, M.F. Gurish, K.F. Austen, R.L. Stevens, Transcriptional regulation of the mucosal mast cell-specific protease gene, MMCP-2, by interleukin 10 and interleukin 3, J. Biol. Chem. 267, (1992) 8473–8477.

[40] K.K. Eklund, N. Ghildyal, K.F. Austen, R.L. Stevens, Induction by IL-9 and suppression by IL-3 and IL-4 of the levels of chromosome 14-derived transcripts that encode late-expressed mouse mast cell proteases, J. Immunol. 151, (1993) 4266–4273.

[41] T. Tsujimura, T. Furitsu, M. Morimoto, K. Isozaki, S. Nomura, Y. Matsuzawa, Y. Kitamura, Y. Kanakura, Ligand-independent activation of c-kit receptor tyrosine kinase in a murine mastocytoma cell line P-815 generated by a point mutation, Blood 83, (1994) 2619–2626.

[42] L. Miller, G.Alber, N. Varin-Blank, R. Ludowyke, H. Metzger, Transmembrane signaling in P815 mastocytoma cells by transfected IgE receptors, J. Biol. Chem. 265, (1990) 12444–12453.

[43] U. Blank, C. Ra, L. Miller, K. White, H. Metzger, J.P. Kinet, Complete structure

and expression in transfected cells of high affinity IgE receptor, Nature 337, (1989) 187–189.

[44] M. Plaut, J.H. Pierce, C.J. Watson, J. Hanley-Hyde, R.P. Nordan, W.E.Paul, Mast cell lines produce lymphokines in response to cross-linkage of FcεRI or to calcium ionophores, Nature 339, (1989) 64–67.

[45] A.Wodnar-Filipowicz, C.H. Heusser, C. Moroni, Production of the haemopoietic growth factors GM-CSF and interleukin-3 by mast cells in response to IgE receptor-mediated activation, Nature 339, (1989) 150–152.

[46] J.R. Gordon, S.J. Galli, Mast cells as a source of both preformed and immunologically inducible TNF-alpha/cachectin, Nature 346, (1990) 274–276.

[47] P.R. Burd, W.C. Thompson, E.E. Max, F.C. Mills, Activated mast cells produce interleukin 13, J. Exp. Med. 181, (1995) 1373–1380.

[48] T.R. Hundley, A.R. Prasad, M.A. Beaven, Elevated levels of cyclooxygenase-2 in antigen-stimulated mast cells is associated with minimal activation of p38 mitogen-activated protein kinase, J. Immunol. 167, (2001) 1629–1636.

[49] M. Murakami, C.O. Bingham, 3rd, R. Matsumoto, K.F. Austen, J.P. Arm, IgE-dependent activation of cytokine-primed mouse cultured mast cells induces a delayed phase of prostaglandin D_2 generation via prostaglandin endoperoxide synthase-2, J. Immunol. 155, (1995) 4445–4453.

[50] M. Murakami, R. Matsumoto, K.F. Austen, J.P. Arm, Prostaglandin endoperoxide synthase-1 and -2 couple to different transmembrane stimuli to generate prostaglandin D_2 in mouse bone marrow-derived mast cells, J. Biol. Chem. 269, (1994) 22269–22275.

[51] R. Kawata, S.T. Reddy, B. Wolner, H.R. Herschman, Prostaglandin synthase 1 and

prostaglandin synthase 2 both participate in activation-induced prostaglandin D_2 production in mast cells, J. Immunol. 155, (1995) 818–825.

[52] E. Razin, J.M. Mencia-Huerta, R.L. Stevens, R.A. Lewis, F. T. Liu, E. Corey, K.F. Austen, IgE-mediated release of leukotriene C_4, chondroitin sulfate E proteoglycan, beta-hexosaminidase, and histamine from cultured bone marrow-derived mouse mast cells, J. Exp. Med. 157, (1983) 189–201.

[53] K. Farhat, S. Riekenberg, H. Heine, J. Debarry, R. Lang, J. Mages, U. Buwitt-Beckmann, K. Röschmann, G. Jung, K.H. Wiesmüller, A.J. Ulmer, Heterodimerization of TLR2 with TLR1 or TLR6 expands the ligand spectrum but does not lead to differential signaling, J. Leukoc. Biol. 83, (2008) 692–701.

[54] F. Sandor, E. Latz, F. Re, L. Mandell, G. Repik, D.T. Golenbock, T. Espevik, E.A. Kurt-Jones, R.W. Finberg, Importance of extra- and intracellular domains of TLR1 and TLR2 in NFkappa B signaling, J. Cell Biol. 162, (2003) 1099–1110.

[55] J.H. Butterfield, D. Weiler, G. Dewald, G.J. Gleich, Establishment of an immature mast cell line from a patient with mast cell leukemia, Leuk Res. 12, (2003) 345–355.

FIGURE CAPTIONS

Fig. 1. Effect of the DMSO concentration in the freezing medium on the viability of MMCH-D5 cells. The data represent the percentage of living cells in total frozen cells and are expressed as mean ± standard deviation (SD) (n = 3). The different letters indicate significant differences at $P < 0.05$ in Tukey's multiple comparison test.

Fig. 2. Expression profiles of mast cell proteases. Data represent the percentage value relative to GAPDH expression in P815-6TgR cells, IgE-reactive MMCH clones, and BMMCs. Data are expressed as mean ± SD (n = 3).

Fig. 3. Dependency of cell proliferation on IL-3. The cells were seeded at 5×10^4 cells/mL in the absence (control) or presence of 5 ng/mL IL-3, and cell proliferation was measured at 24, 48, 72, and 96 h. Data are expressed as mean ± SD (n = 3).

Fig. 4. Expression of FcεRI. (**A**) Intracellular mRNA expression of FcεRI α, β, and γ subunits in P815-6TgR cells, IgE-reactive MMCH clones, and BMMCs. (**B**) Cell surface expression of FcεRIα protein. The numbers in the upper-right plot indicate the percentage of the sorted cell population in the quadrant.

Fig. 5. Transmission electron micrographs. Transmission electron micrographs of P815-6TgR cells (**A**), MMCH-D5 cells (**B**, **C**, and **D**), and BMMCs (**E** and **F**). Bars indicate 5 μm (**C**), 2 μm (**A**, **B**, and **E**), and 1 μm (**D** and **F**).

Fig. 6. Degranulation and histamine release. β-Hexosaminidase activity of the

supernatants from P815-6TgR and MMCH-D5 cells stimulated with a 2-fold-dilution series of concentrations of IgE + 10 ng/mL DNP-HSA (**A**) and with 5 μg/mL IgE + 10-fold-dilution series of concentrations of DNP-HSA (**B**). Data represent the percentage relative to total β-hexosaminidase activity and are expressed as mean ± SD (n = 3). $^{**}P < 0.01$ and $^{***}P < 0.001$ vs. unstimulated MMCH-D5 cells (Student's *t*-test). (**C**) Histamine released into MMCH-D5 supernatants after 1 h stimulation with 5 μg/mL IgE and 10 ng/mL DNP-HSA. Data are expressed as mean ± SD (n = 3). $^{**}P < 0.01$ vs. unstimulated cells (Student's *t*-test).

Fig. 7. Expression of proinflammatory genes and production of lipid mediators. (**A**) Intracellular mRNA expression induced by stimulation with 1 μg/mL IgE + 10 ng/mL DNP-HSA. Data represent the percentage relative to unstimulated cells and are expressed as mean ± SD (n = 3). $^{**}P < 0.01$ and $^{***}P < 0.001$ vs. unstimulated cells (Student's *t*-test). (**B**) PGD_2 released into MMCH-D5 supernatant after 1 and 6 h of stimulation with 1 μg/mL IgE + 100 ng/mL DNP-HSA. Data are expressed as mean ± SD (n = 3). $^{***}P < 0.001$ vs. unstimulated cells (Student's *t*-test). (**C**) LTC_4 released into MMCH-D5 supernatants after 1 h stimulation with 1 μg/mL IgE + 100 ng/mL DNP-HSA. Data are expressed as mean ± SD (n = 3). ***$P < 0.001$ vs. unstimulated cells (Student's *t*-test).

Fig. 8. Expression and function of TLRs. (**A**) Expression of TLRs in P815-6TgR cells, MMCH clones, and BMMCs. (**B**) Induction of TNF-α expression in MMCH-D5, BMMCs, and P815-6TgR cells after treatments with Pam_3CSK_4 and LPS. Data represent the percentage relative to that of unstimulated cells and are expressed as mean

± SD (n = 3). $^{***}P < 0.001$ vs. unstimulated MMCH-D5 cells. $^{\#}P < 0.05$ and $^{\#\#}P < 0.01$ vs. unstimulated BMMCs (Student's *t*-test).

Fig. 1

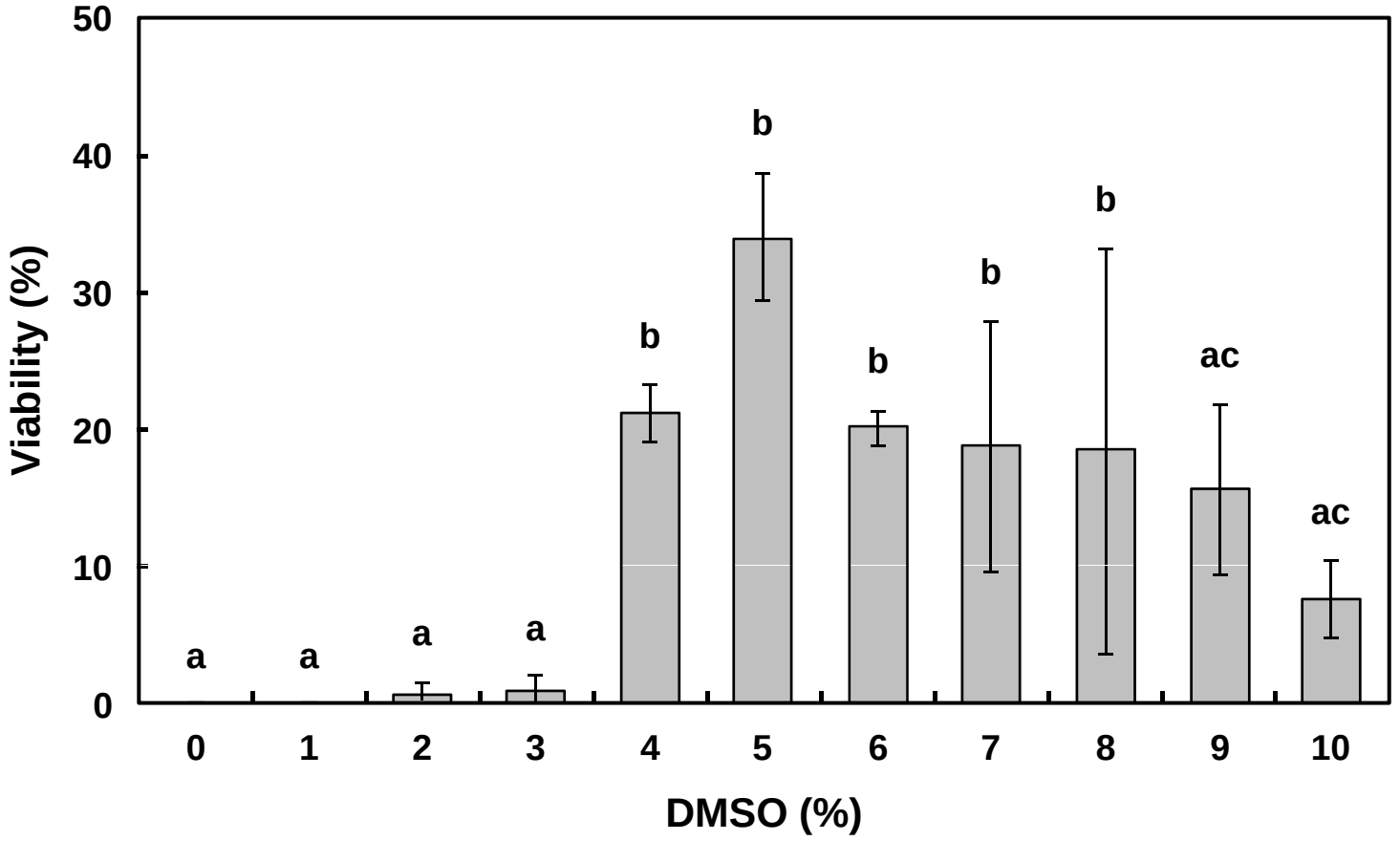

Fig. 2

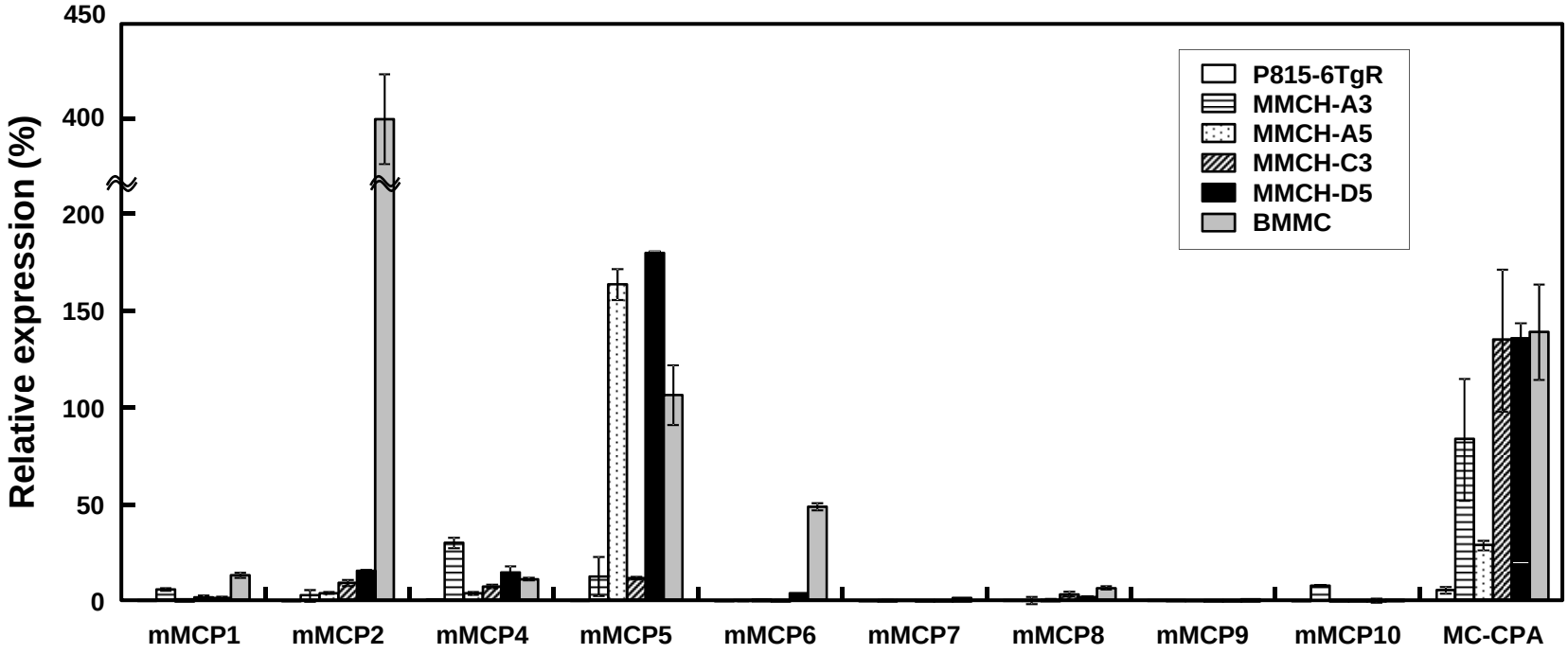
Relative expression (%)
450
400
200
150
100
50
0
P815-6TgR
MMCH-A3
MMCH-A5
MMCH-C3
MMCH-D5
BMMC
mMCP1
mMCP2
mMCP4
mMCP5
mMCP6
mMCP7
mMCP8
mMCP9
mMCP10
MC-CPA

Fig. 3

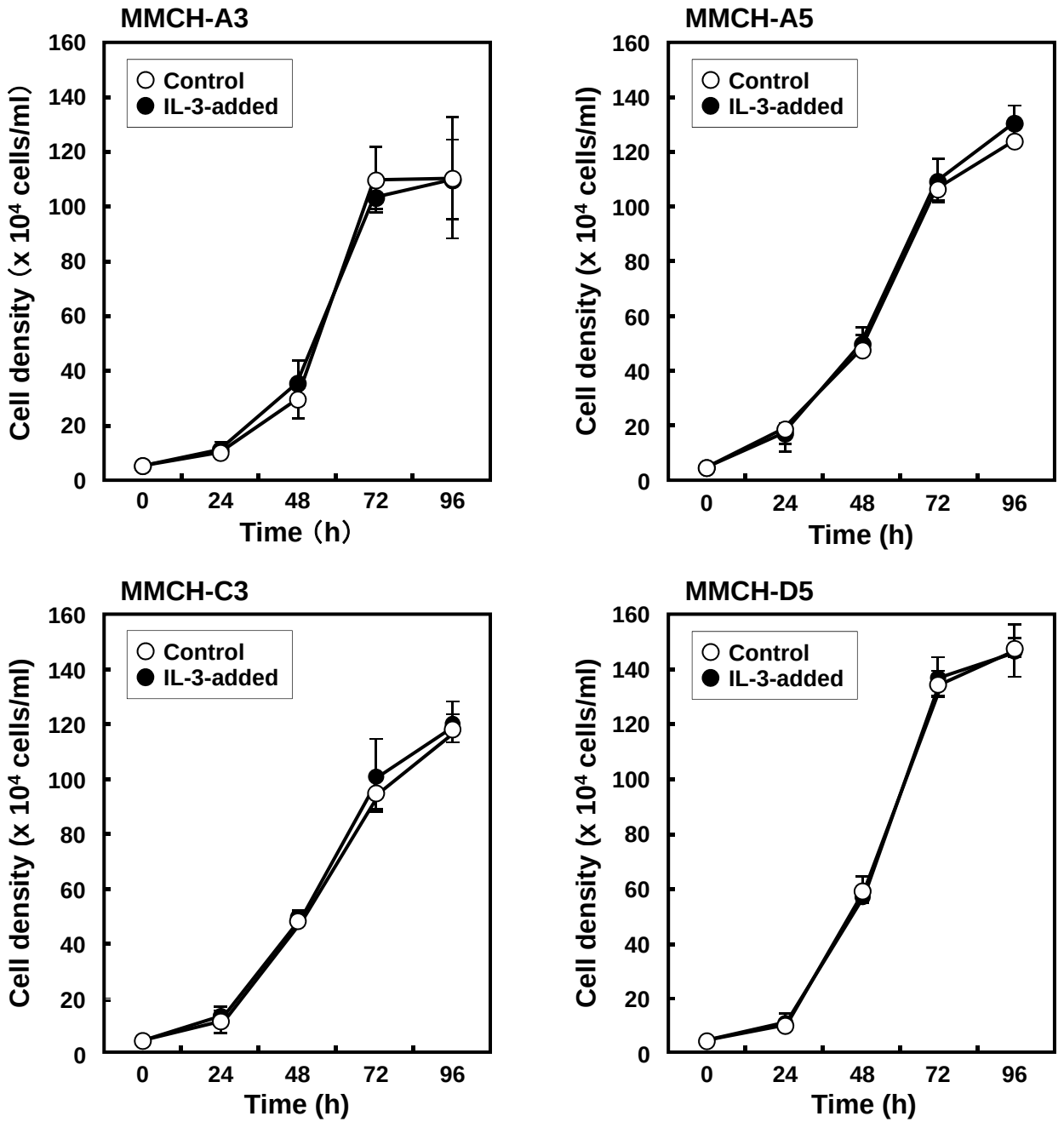
MMCH-A3
MMCH-A5
MMCH-C3
MMCH-D5
Control
IL-3-added
Cell density (x 10⁴ cells/ml)
Time (h)
0
20
40
60
80
100
120
140
160
0
24
48
72
96

Fig. 4

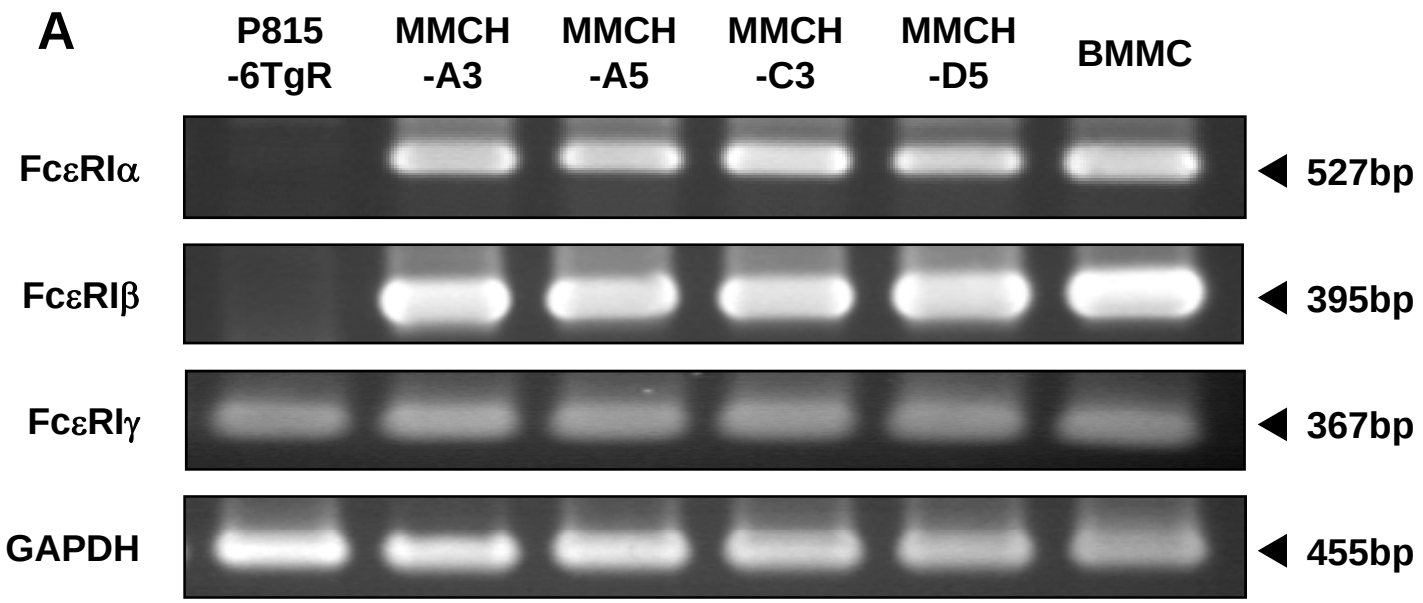
A
P815 -6TgR
MMCH -A3
MMCH -A5
MMCH -C3
MMCH -D5
BMMC
FcεRIα
FcεRIβ
FcεRIγ
GAPDH
527bp
395bp
367bp
455bp

Fig. 4 B

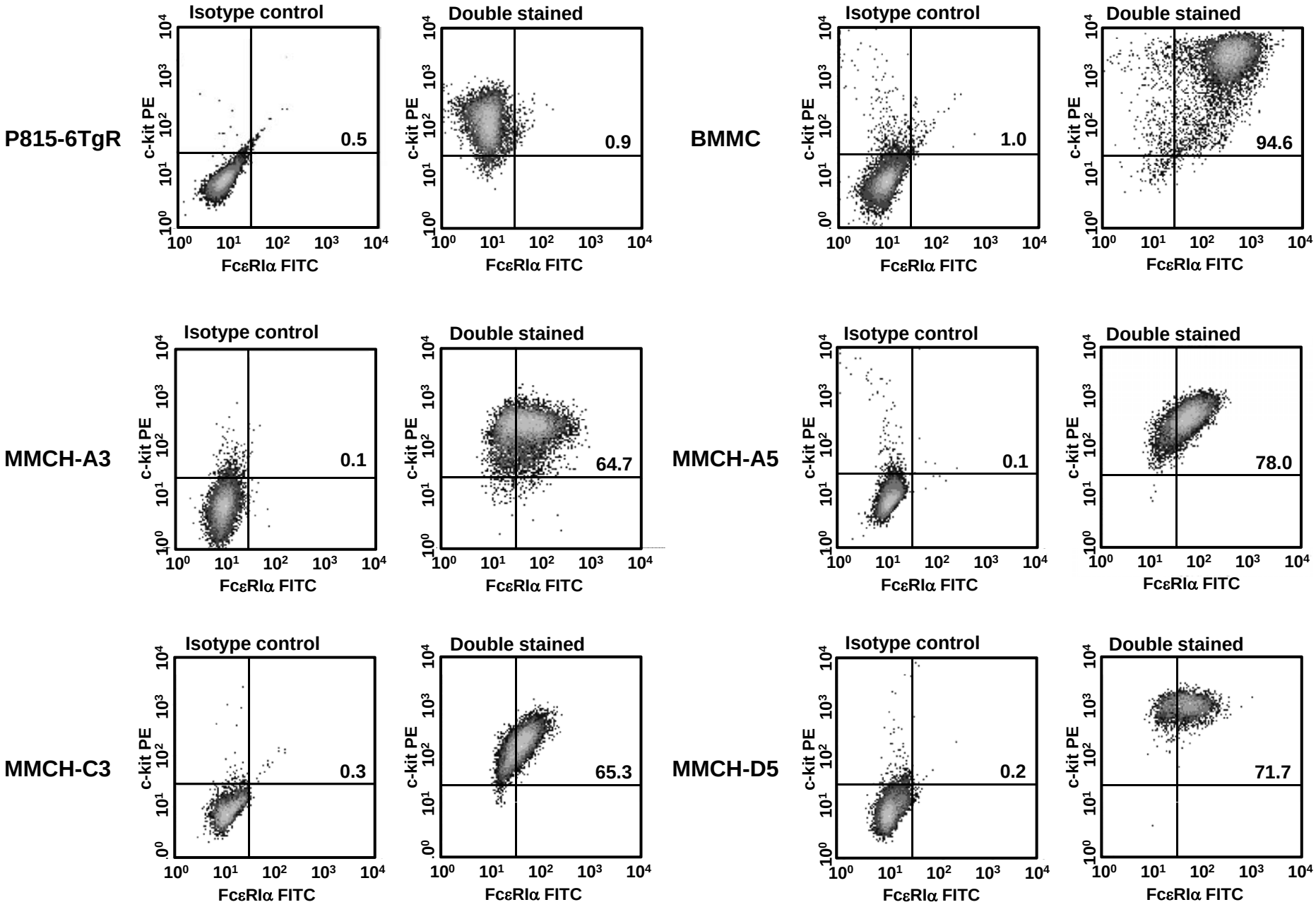
P815-6TgR
Isotype control
Double stained
0.5
0.9
BMMC
1.0
94.6
MMCH-A3
0.1
64.7
MMCH-A5
0.1
78.0
MMCH-C3
0.3
65.3
MMCH-D5
0.2
71.7
c-kit PE
FcεRIα FITC

Fig. 5

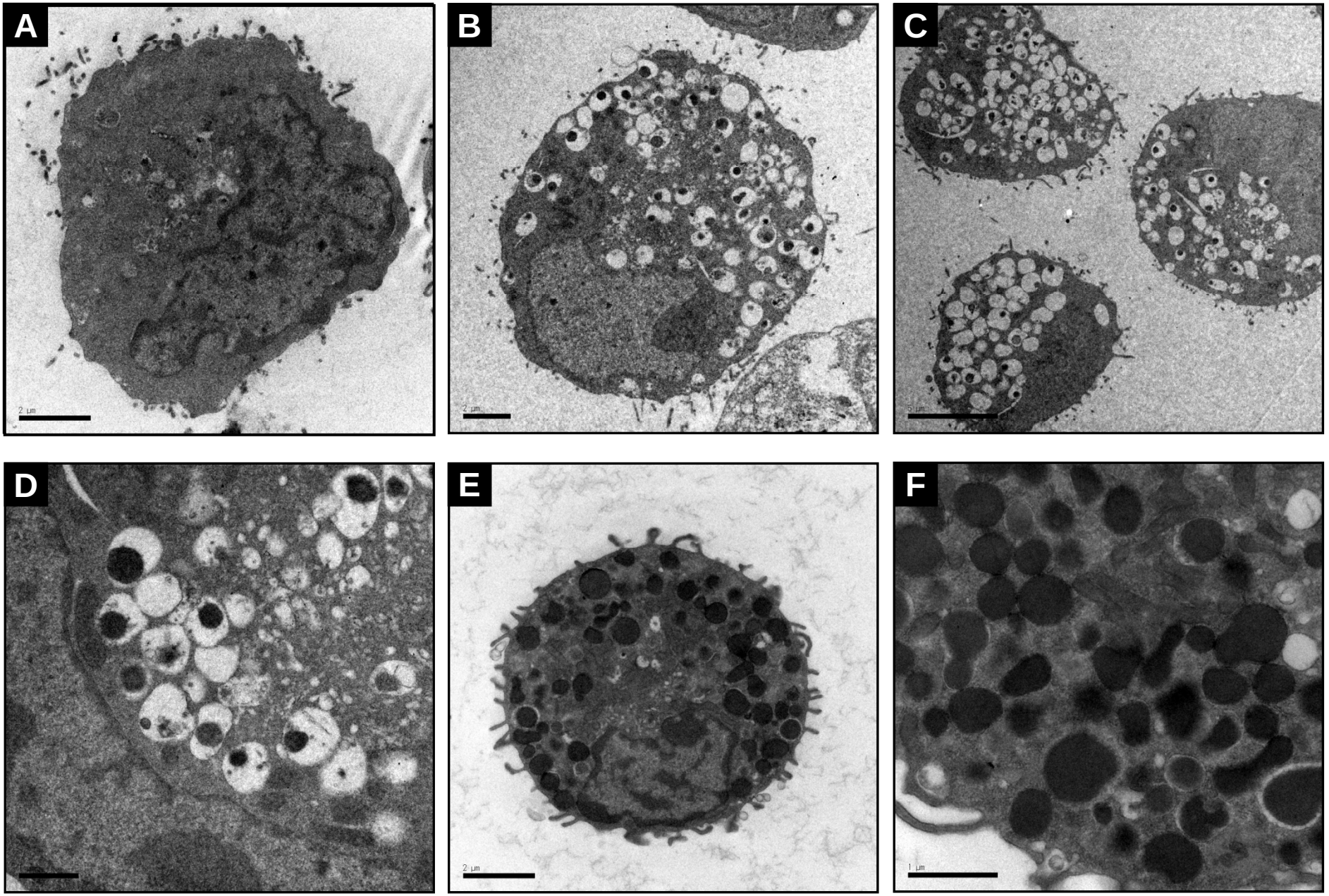

Fig. 6

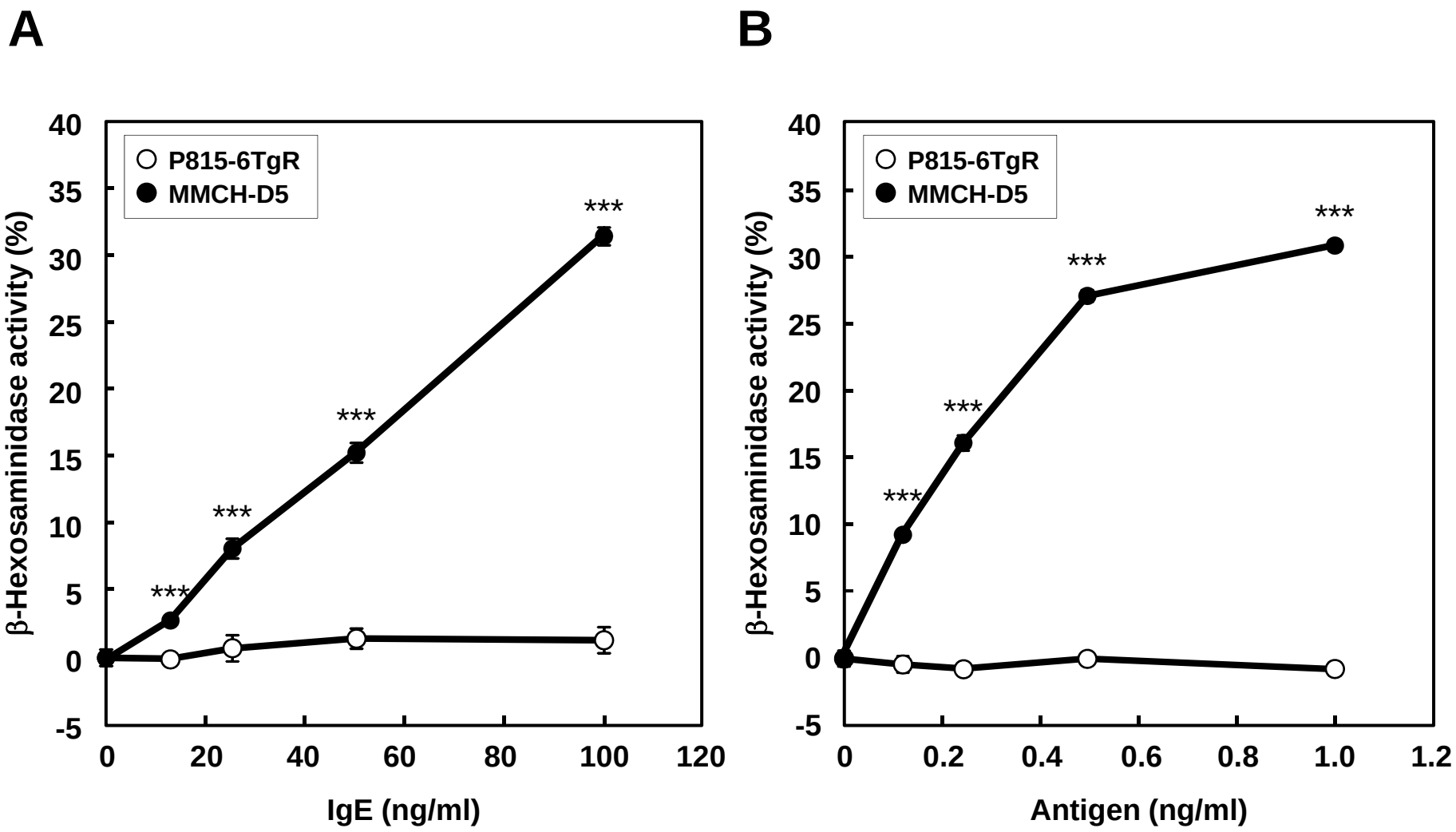
A
B
P815-6TgR
MMCH-D5
β-Hexosaminidase activity (%)
IgE (ng/ml)
Antigen (ng/ml)
***
40
35
30
25
20
15
10
5
0
-5
0
20
40
60
80
100
120
0.2
0.4
0.6
0.8
1.0
1.2

Fig. 6

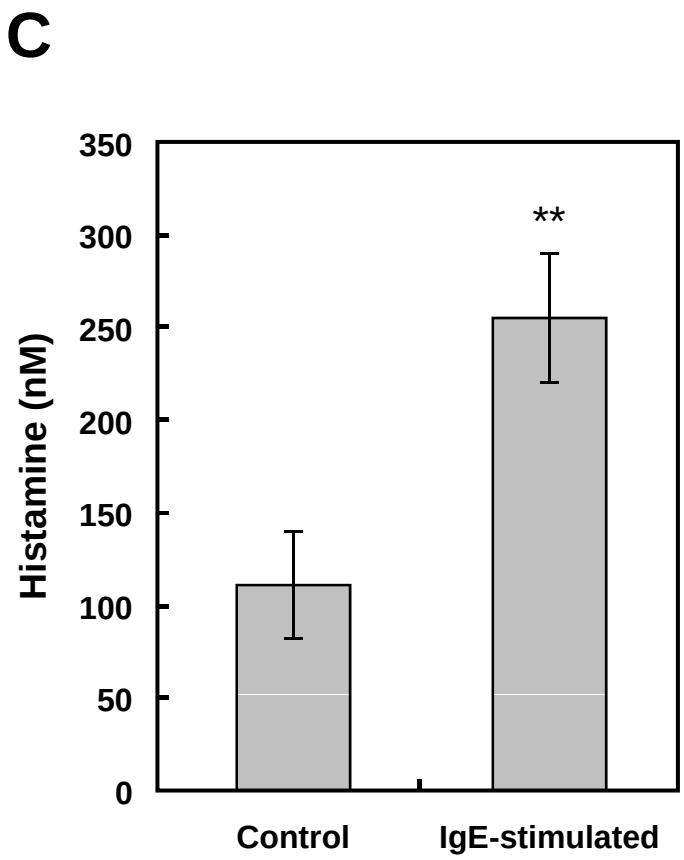
C
Histamine (nM)
350
300
250
200
150
100
50
0
**
Control
IgE-stimulated

Fig. 7

A

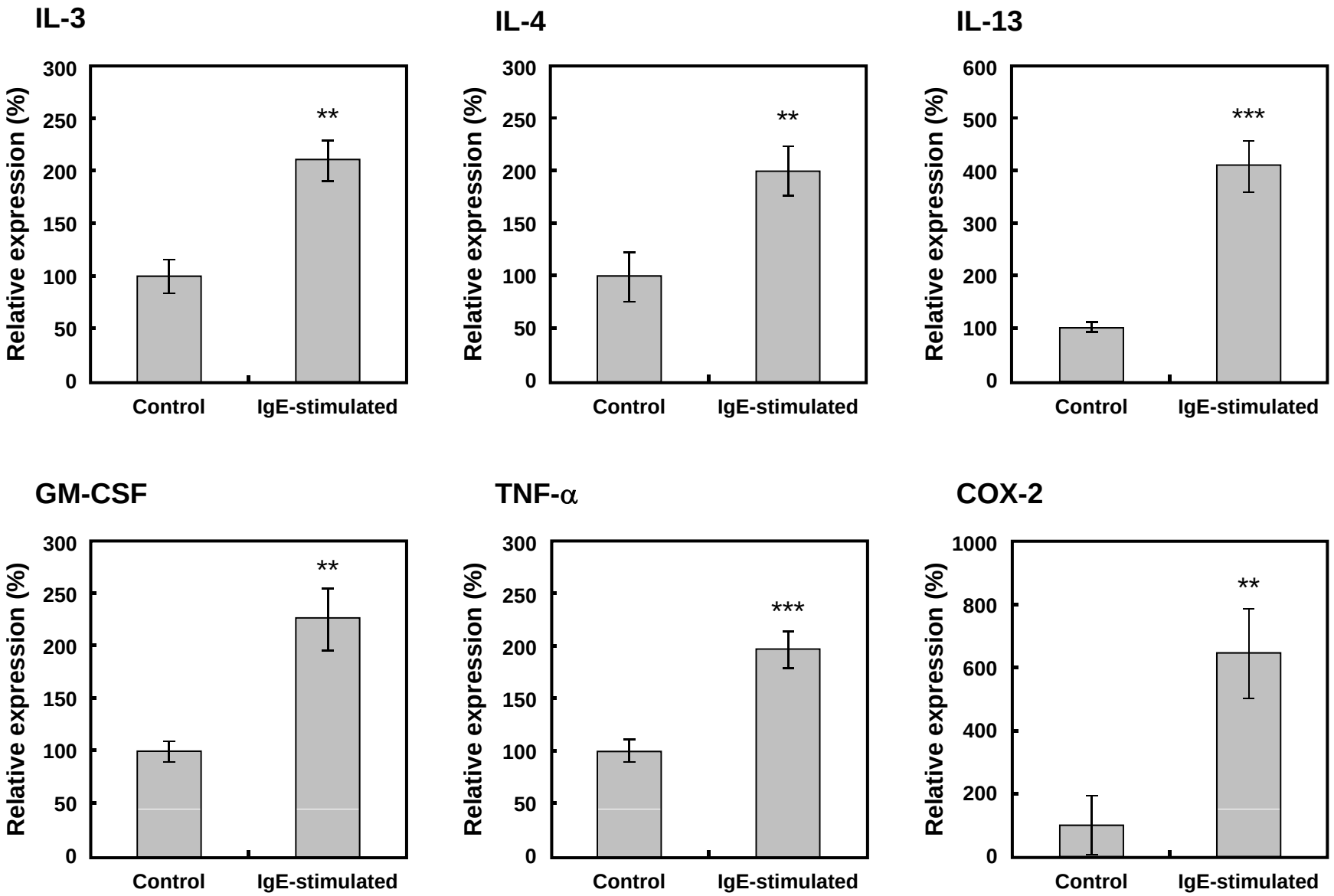
IL-3
Relative expression (%)
300
250
200
150
100
50
0
**
Control
IgE-stimulated
IL-4
Relative expression (%)
300
250
200
150
100
50
0
**
Control
IgE-stimulated
IL-13
Relative expression (%)
600
500
400
300
200
100
0
***
Control
IgE-stimulated
GM-CSF
Relative expression (%)
300
250
200
150
100
50
0
**
Control
IgE-stimulated
TNF-α
Relative expression (%)
300
250
200
150
100
50
0
***
Control
IgE-stimulated
COX-2
Relative expression (%)
1000
800
600
400
200
0
**
Control
IgE-stimulated

Fig. 7

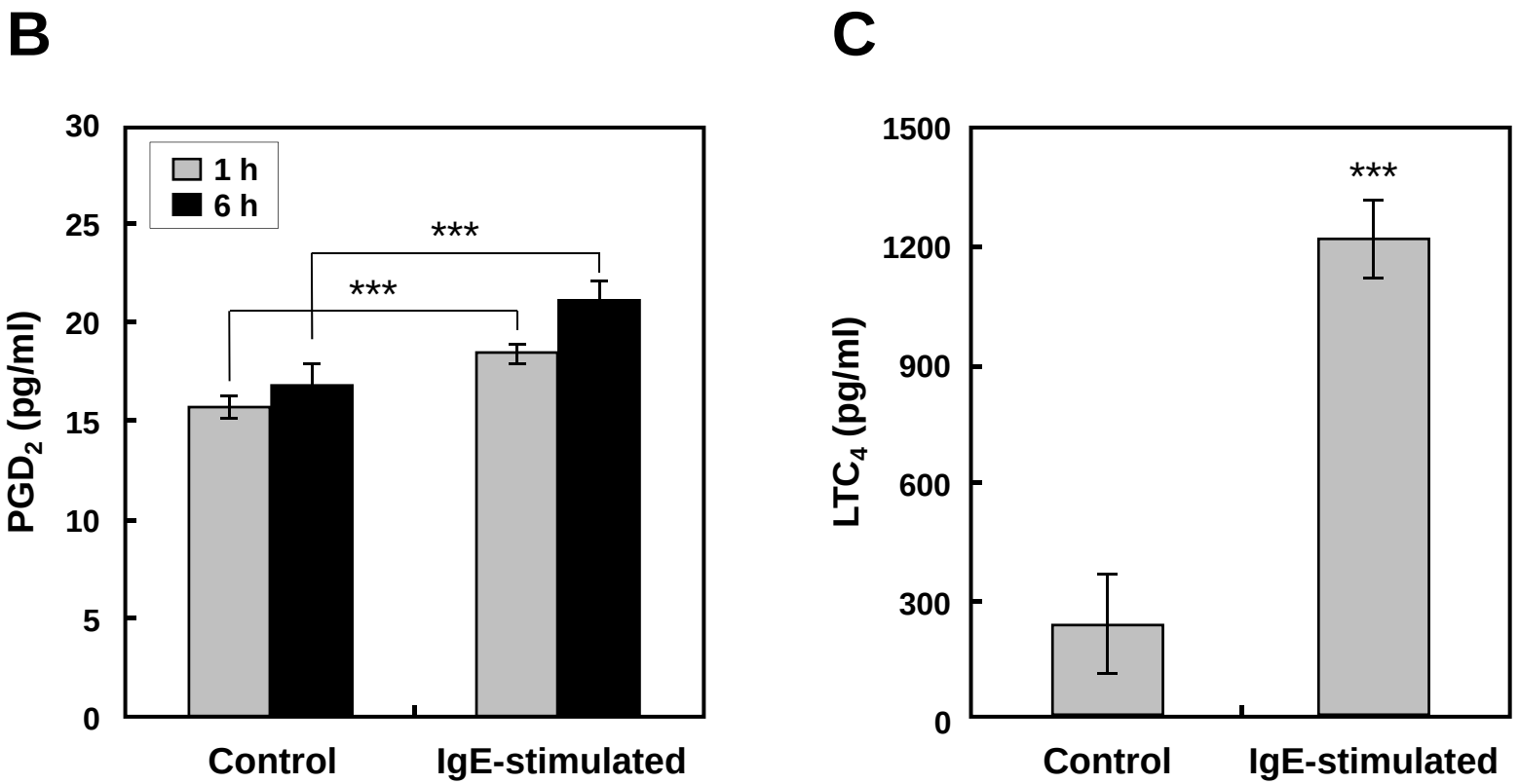
B
30
25
20
15
10
5
0
PGD2 (pg/ml)
1 h
6 h
***
***
Control
IgE-stimulated
C
1500
1200
900
600
300
0
LTC4 (pg/ml)
***
Control
IgE-stimulated

Fig. 8

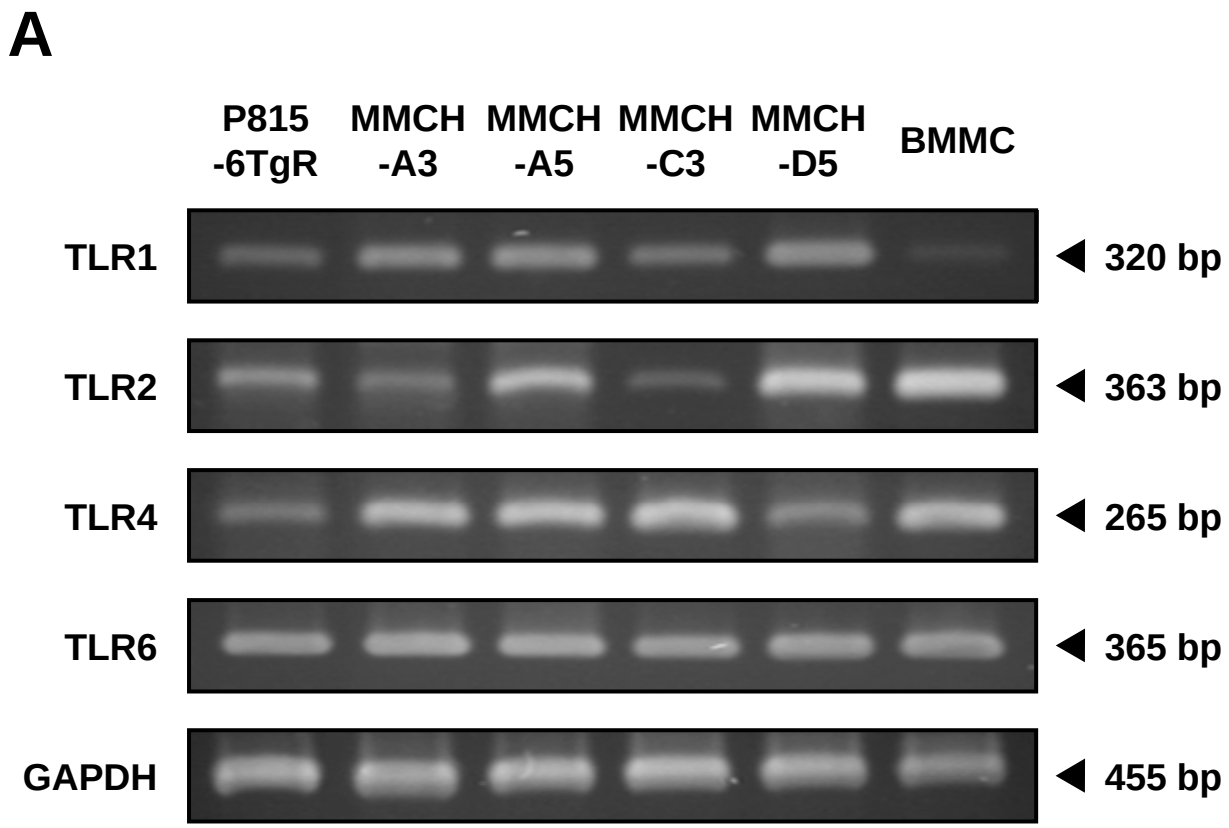
A
P815 -6TgR
MMCH -A3
MMCH -A5
MMCH -C3
MMCH -D5
BMMC
TLR1
320 bp
TLR2
363 bp
TLR4
265 bp
TLR6
365 bp
GAPDH
455 bp

Fig. 8

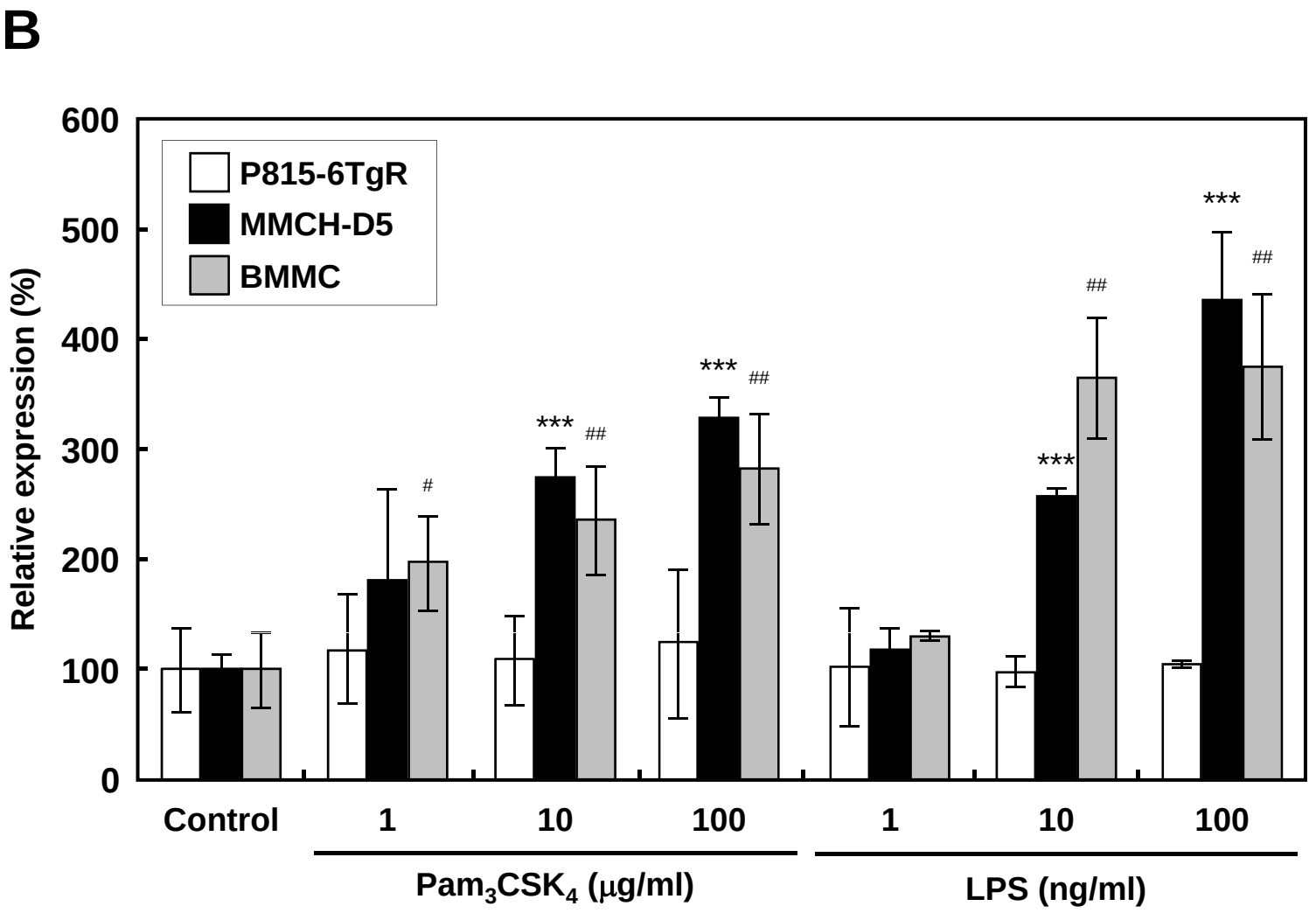
B
P815-6TgR
MMCH-D5
BMMC
Relative expression (%)
600
500
400
300
200
100
0
Control
1
10
100
1
10
100
Pam3CSK4 (μg/ml)
LPS (ng/ml)
#
***
##